Acoustic modal analysis experiment

Jeffrey J. Nieter and Rajendra Singh
Department of Mechanical Engineering, The Ohio State University, 206 W. 18th Avenue, Columbus, Ohio 43210

(Received 8 January 1982; accepted for publication 16 March 1982)

This paper proposes an experimental modal technique for acoustic ducts, mufflers, and resonators over the plane-wave frequency regime. Global modal properties, such as natural frequencies and modes of gas oscillation, are extracted from the coincident-quadrature response curves of measured cross-point acoustic impedances at a number of observation locations. The acoustic system is excited by a vibrating piston which is driven by an electromagnetic shaker with bandlimited binary random noise signal. The acoustic impedance is determined using the following two transducers: (i) an accelerometer attached to the piston—its signal is processed to yield volume velocity information, and (ii) a microphone traverse. Digital data acquisition and processing techniques are used to generate the necessary impedance data at a number of locations for modal analysis. In order to demonstrate the validity of our experimental technique, we have applied it to the following example cases, and obtained excellent correlation between theory and experiment: closed–closed tube, closed–open tube, and symmetrical and unsymmetrical lumped parameter systems. In this paper, we discuss the conceptual, analytical, physical, and measurement considerations of the acoustic modal analysis. We also point out some areas of further research.

PACS numbers: 43.85.Bh, 43.20.Ks, 43.85.Kr

INTRODUCTION

Experimental modal analysis is the process of extracting dynamic characteristics, such as natural frequencies, mode shapes, and modal parameters from the transfer functions measured at a finite number of observation points. In the discipline of mechanical vibrations/structural dynamics, modal analysis is now being used widely for the following potential applications: system identification, vibration troubleshooting and diagnostics, development and refinement of mathematical models, etc.[1–10] The modal analysis technique has also been applied to structures radiating noise using an accelerometer or a microphone along with an instrumented hammer.[11,12] In engineering acoustics, and especially duct acoustics, such experimental modal analysis techniques are yet to be developed.

Acoustic duct theory, in several aspects, follows the disciplines of structural vibrations and electrical transmission lines. However, unlike these disciplines, acoustics poses a fundamental measurement problem: out of the two primary variables, pressure (p) and volume velocity (Q), only pressure can be measured accurately and reliably (using a microphone or a very sensitive pressure transducer); conversely, a volume velocity or particle velocity transducer is not available. This problem has forced many investigators over the years to devise indirect means of measuring volume velocity, acoustic impedance, and other inherent acoustic characteristics. A critical review of the literature on acoustic impedance measurement methods is available in Ref. 13. Perhaps the most common impedance method is the standing wave tube method.[14] This method uses a traversing microphone to determine the location and magnitude of successive maxima and minima of the standing wave patterns in a tube terminated by an unknown duct system or acoustic material. From this information, input impedance, reflection and absorption coefficients, etc. can be calculated. However, this standing wave tube method cannot be readily used to determine acoustic natural frequencies and mode shapes. Also, this method has a number of inherent limitations which make it unattractive for modal analysis work.[13]

Theoretically, the response of a linear system can be formulated using the modal expansion approach. Thus if we take a number of pressure measurements in a duct, we should be able to extract natural frequencies and mode shapes from the measured data. This has been demonstrated by Moore for radial and circumferential modes in fan ducts.[15] However, this technique may suffer from the following limitations: (i) prior knowledge of eigenvalues and eigenvectors may be required, (ii) an extremely large number of measurement locations are needed to generate a data set even for the first few modes, (iii) a matrix inversion scheme or any other suitable numerical procedure is generally too cumbersome for general applications, and finally (iv) the information obtained using this method may be incomplete. Therefore a more direct modal analysis technique, very similar to the method currently used in solid mechanics, should be developed. This paper undertakes such a task for application to acoustic ducts, mufflers, and resonators. In this paper we restrict our method to only the plane-wave frequency regime, and our interest is mainly focused on the global properties such as natural frequencies and modes of gas oscillation.

I. THEORY

The first question we ask ourselves is: why can't we use the experimental modal analysis techniques and computer software currently being used for structures and mechanical systems? To answer this question we examine the difference between mechanical systems (often dispersive) and acoustic systems (often nondispersive). In solid mechanics, several kinematic and dynamic types of transducers are available; thus the measurement of any conceivable transfer function is possible. The same is not true for acoustics where only one measurement, pressure, can be conducted, and therefore only a limited number of transfer functions can be measured. While solids are generally restrained, acoustic systems may be unrestrained. One more major difference is in the excitation type: solids are generally force driven, while the acoustic systems are generally motion driven (e.g., fluid injection, vibrating piston, etc.). In short, the question now is: how do we apply the techniques developed for dispersive, restrained, and force-excited elastic systems to nondispersive, unrestrained, and motion-excited elastic systems? A study of this depth is obviously beyond the scope of our paper. Nevertheless, we will present an approach for acoustic modal analysis which may be able to use the same equipment hardware and computer software currently used for mechanical systems.

Consider an acoustic duct system in the plane-wave frequency regime with ω_u, rad/s as the upper frequency limit. To develop acoustic modal analysis theory we assume the following: (i) an isotropic and perfectly elastic fluid medium with zero mean fluid flow, (ii) a linear dynamic system and reciprocity relationship, (iii) a lightly damped (viscous) system, and (iv) light modal overlapping with only one mode at each natural frequency.

Consider an n-dimensional acoustic duct system where n measurement locations are spatially distributed so as to cover the dynamic characteristics over a frequency range of $0 - \omega_u$, rad/s. We can describe the inherent characteristics of the acoustic system with the acoustic impedance (Z) matrix — an $n \times n$ matrix:

$$\{\tilde{p}(\tilde{s})\} = [\tilde{Z}(\tilde{s})]\{\tilde{Q}(\tilde{s})\}, \tag{1}$$

where s is the Laplace variable and the tilde over a symbol implies that it is a complex quantity. Considering $\{\tilde{Q}(\tilde{s})\}$ to be the excitation and $\{\tilde{p}(\tilde{s})\}$ to be the response, we define the admittance (Y) matrix as

$$[\tilde{Y}(\tilde{s})]\{\tilde{p}(\tilde{s})\} = \{\tilde{Q}(\tilde{s})\}, \tag{2}$$

where

$$[\tilde{Y}(\tilde{s})] = [\tilde{Z}(\tilde{s})]^{-1}. \tag{3}$$

The Eigenvalue solution is given by the roots of the characteristic equation:

$$|\tilde{Y}(\tilde{s})| = 0. \tag{4}$$

We get n pairs of distinct roots or poles (s_r):

$$\tilde{s}_r = -\zeta_r\omega_r + j\omega_{rd},$$
$$\tilde{s}_r^* = -\zeta_r\omega_r - j\omega_{rd}, \quad r = 1,2,\ldots,n, \tag{5}$$

where r is the modal index, ζ_r is the modal damping ratio, ω_r is the natural frequency (rth mode), ω_{rd} is the damped natural frequency (rth mode), and superscript * signifies complex conjugate.

The mode of oscillation (ψ_r) is given by

$$[\tilde{Y}(\tilde{s}_r)]\{\tilde{\psi}_r\} = \{0\}. \tag{6}$$

Note that $\tilde{\psi}_r$ is the pressure mode shape.

We can express $[\tilde{Z}]$ in the partial fraction form as

$$[\tilde{Z}(\tilde{s})] = \sum_{r=1}^{n}\left(\frac{[\tilde{A}_r]}{\tilde{s}-\tilde{s}_r} + \frac{[\tilde{A}_r^*]}{\tilde{s}-\tilde{s}_r^*}\right) + [\tilde{Z}(\tilde{s})]_u, \tag{7}$$

where $[\tilde{A}_r]$ is the complex residue matrix ($n \times n$) for the rth mode, and $[\tilde{Z}(\tilde{s})]_u$ is the upper residual term for $r = n+1, n+2,\ldots,\infty$. We can relate $[\tilde{A}_r]$ to $\tilde{\psi}_r$ as[4]

$$[\tilde{A}_r] = \alpha_r\{\tilde{\psi}_r\}\{\tilde{\psi}_r\}^T, \tag{8}$$

where α_r is the scaling constant and superscript T indicates the transpose.

For our analysis, we assume that $[\tilde{Z}(\tilde{s})]_u \simeq 0$. Normally $[\tilde{Z}(\tilde{s})]$ is only measured for positive frequencies and therefore the impedance matrix $[\tilde{Z}_r(\tilde{s})]$ for the rth mode is given by the following expression:

$$[\tilde{Z}_r(\tilde{s})] \simeq [\tilde{A}_r]/(\tilde{s}-\tilde{s}_r) = ([B_r] + j[D_r])/(\tilde{s}-\tilde{s}_r), \tag{9}$$

where

$$B_r = \mathrm{Re}(\tilde{A}_r), \quad D_r = \mathrm{Im}(\tilde{A}_r). \tag{10}$$

Acoustic impedance in the frequency domain is given by substituting $j\omega$ for $\tilde{s}$ and assuming $\omega_r \simeq \omega_{rd}$ as the ζ_r values were assumed to be very small. Thus $[\tilde{Z}_r(\omega)]$ is

$$[\tilde{Z}_r(\omega)] = \mathrm{Re}\{[\tilde{Z}_r(\omega)]\} + j\,\mathrm{Im}\{[\tilde{Z}_r(\omega)]\}$$
$$= ([B_r] + j[D_r])/[\zeta_r\omega_r + j(\omega - \omega_r)] \tag{11}$$

$$\mathrm{Re}\{[\tilde{Z}_r(\omega)]\} = \frac{[B_r]\zeta_r\omega_r + [D_r](\omega-\omega_r)}{(\zeta_r\omega_r)^2 + (\omega-\omega_r)^2} \tag{12a}$$

$$\mathrm{Im}\{[\tilde{Z}_r(\omega)]\} = \frac{[D_r]\zeta_r\omega_r - [B_r](\omega-\omega_r)}{(\zeta_r\omega_r)^2 + (\omega-\omega_r)^2}. \tag{12b}$$

At resonance ($\omega = \omega_r$) we get

$$\mathrm{Re}\{[\tilde{Z}_r(\omega)]\} = [B_r]/(\zeta_r\omega_r)$$
$$\mathrm{Im}\{[\tilde{Z}_r(\omega)]\} = [D_r]/(\zeta_r\omega_r). \tag{13}$$

For a lightly damped system, the mode or residue is almost real valued[1,4]

$$[D_r] \simeq [0]. \tag{14}$$

Thus

$$\mathrm{Im}\{[\tilde{Z}_r(\omega)]\} \simeq [0] \tag{15a}$$

and

$$\mathrm{Re}\{[\tilde{Z}_r(\omega)]\} = [B_r]/(\zeta_r\omega_r)$$
$$= \mathrm{Re}(\alpha_r\{\tilde{\psi}_r\}\{\tilde{\psi}_r\}^T)/(\zeta_r\omega_r). \tag{15b}$$

Note that we can also expand $[\tilde{Z}_r(\tilde{s})]$ in the following form, in addition to Eq. (9):

$$[\tilde{Z}'_r(\tilde{s})] \simeq j[\tilde{A}_r]/(\tilde{s}-\tilde{s}_r) = (-[D_r] + j[B_r])/(\tilde{s}-\tilde{s}_r), \tag{16}$$

where B_r and D_r are given by Eq. (10). For a lightly damped system ($[D_r] \simeq [0]$) at resonance ($\omega = \omega_r$), we get

$$\mathrm{Re}\{[\tilde{Z}'_r(\omega)]\} \simeq [0], \tag{17a}$$

$$\mathrm{Im}\{[\tilde{Z}'_r(\omega)]\} = [B_r]/(\zeta_r\omega_r)$$
$$= \mathrm{Im}(\alpha_r\{\tilde{\psi}_r\}\{\tilde{\psi}_r\}^T)/(\zeta_r\omega_r). \tag{17b}$$

Thus coincident-quadrature responses of acoustic impedance are given by Eqs. (15) and (17). We note that these are mutually orthogonal sets; only one set exists at a given ω_r for any acoustic system. (This is not unique to acoustic systems;

such sets are also found in mechanical systems. The reasons and predictions of such orthogonal sets are beyond the scope of our study here.) The steps for determining ω_r and ψ_r are as follows: (i) determine which set exists at a given resonance [i.e., either Eq. (15) or Eq. (17) is valid but not both], (ii) if $\mathrm{Im}\{[\tilde{Z}_r(\omega)]\}\simeq[0]$, then find ω_r from quadrature response spectrum, and determine ψ_r using coincident response spectrum—$\mathrm{Re}\{[\tilde{Z}_r(\omega)]\}$, or (iii) if $\mathrm{Re}\{[\tilde{Z}'_r(\omega)]\}\simeq[0]$, then find ω_r from the coincident response spectrum, and determine ψ_r using quadrature response spectrum—$\mathrm{Im}\{[\tilde{Z}'_r(\omega)]\}$. Do we have to measure the complete impedance matrix $[\tilde{Z}_r(\omega)]$ for the determination of ω_r and ψ_r? The answer is no because any row or column will contain sufficient information. Therefore for acoustic impedance measurements we can excite the system at a single point, i.e., all the terms in $\{\tilde{Q}\}$ are zero except one, say $\tilde{Q}_1$. Also, we may utilize the reciprocity relationship, $\tilde{Z}_{ik}=\tilde{Z}_{ki}$, for obtaining the necessary impedance data. Thus for an n-dimensional system we need to measure $\{\tilde{p}\}$ and $\tilde{Q}_1$; note that at any given location in the system, $\tilde{p}_i$ and $\tilde{Q}_1$ must be measured simultaneously.

II. EXPERIMENT

A. Physical and measurements considerations

Figure 1 shows schematically the experimental setup and instrumentation. The acoustic system under study is excited by a known volume velocity source—an electromagnetic shaker-driven piston. The propagated acoustic wave will be a plane-wave front if the following ideal conditions are satisfied: (i) perfect piston driving surface, (ii) rigid duct walls, and (iii) negligible viscous and thermal boundary dissipations at the wall. Realistically speaking, these conditions do not pose any severe limitations and, in general, plane-wave propagation is obtained over a wide frequency range. The validity of measuring acoustic impedance with this method has already been demonstrated by Singh *et al.*[16,17]

Care should be taken in adapting an acoustic duct system for modal analysis testing. The procedure is sensitive to the following physical parameters involved with the experimentation:

(1) Fabrication and fitting of the driving piston should be done with extreme care. Clearance between piston and duct should be minimal so that there is no volume velocity escape through the space between the piston and rigid duct walls. The piston should move well even in the absence of any lubrication. Nevertheless, lubrication with a light grease will not only produce a better seal, but will also reduce the potential for noise radiation from piston and dry duct wall contact. Nonlinear distortion could be induced by either piston wear or misalignment. Also, the piston and connecting rod to the shaker should be such that the dynamics of the piston–rod mechanism is negligible in the frequency range of interest. The piston–rod mechanism should be light enough not to affect the frequency response of the shaker (which incidently should be chosen to have a flat response over the frequency range of interest), but should be heavy and rigid enough relative to the acoustic medium so that a rigid termination of infinite impedance may be assumed.

(2) The end or termination point of the acoustic duct system should be carefully maintained at a known value if checks with an analytical model are to be made. Terminations of either infinite or zero impedance are generally easier to work with.

(3) For measurement in the plane-wave frequency regime, the smallest wavelength of interest should be at least twice the duct diameter. This condition fixes an upper frequency limit.

(4) Piston source and microphone proximity effects could cause some errors.[18] Also, the microphone probe should be properly designed so as not to disturb the acoustic

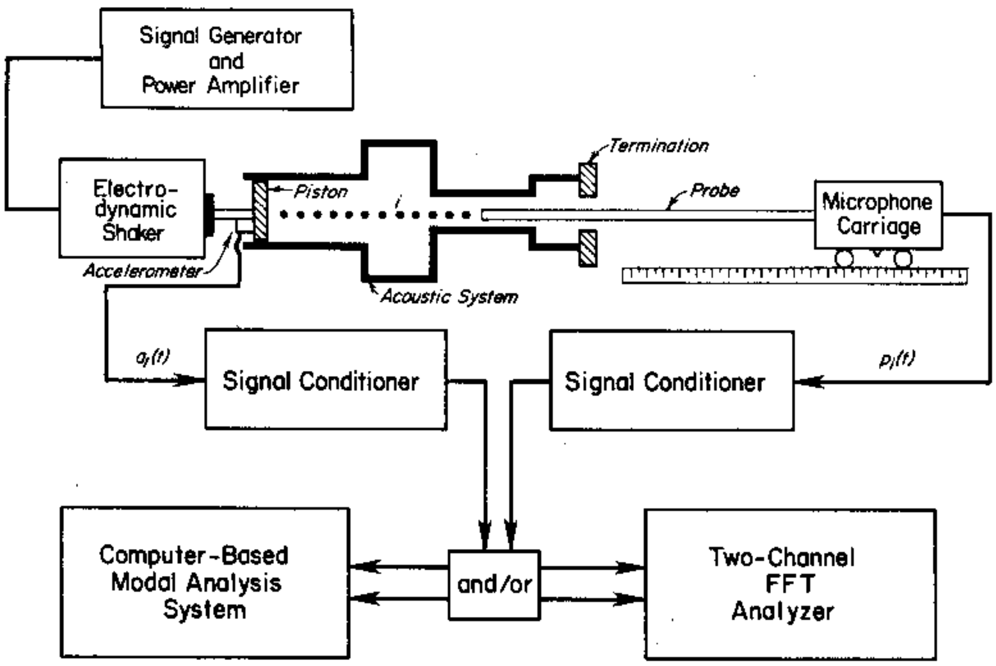

FIG. 1. Schematic representation of the acoustic modal analysis experiment. Some specifications of the instrumentation used are as follows: (i) random noise generator: HP-HOI-3722A, 1.5-kHz bandlimited binary excitation signal; (ii) power amplifier: MB 2120, 125 VA; (iii) electrodynamic shaker: MB-EA1500; (iv) accelerometer: B & K 4344, 2 g, 3.1 pCb/g, Dynamics Instrumentation charge amplifier 7306; (v) microphone system: B & K 4002 standing wave apparatus, B & K 2107 frequency analyzer; and (vi) two-channel FFT analyzer: Nicolet 660A.

field inside the duct.

(5) High ambient noise levels should be avoided; coherence should be monitored to ensure this.

B. Data processing

A digital two-channel frequency analyzer is used to acquire and process data, as shown in Fig. 1. The input volume velocity $Q_1(t)$ is

$$Q_1(t) = S_1 \int a_1(t)dt\,, \tag{18}$$

where S_1 is the cross-sectional area at input ($i = 1$) and $a_1(t)$ is the measured acceleration of the piston. Here we have assumed that acoustic particle velocity is equal to the structural velocity of the piston and that the piston dynamics can be ignored over the frequency range of interest. Since the acoustic impedance is defined in the frequency domain, the discrete Fast Fourier Transform technique is used to convert the signals to the frequency domain.[19,20]

$$\begin{aligned}\tilde{a}_1(\omega) &= \tilde{a}_1(\beta\cdot\Delta\omega)\\ &= \Delta t \sum_{\alpha=0}^{N-1} a_1(\alpha\cdot\Delta t)e^{-j(\beta\cdot\Delta\omega)(\alpha\cdot\Delta t)}\,,\end{aligned} \tag{19a}$$

where N is the total number of time-domain samples, $\Delta\omega$ and Δt are frequency and time resolutions, respectively, $\alpha(\alpha = 0,1,..., N-1)$ is the sample index in the time domain, and $\beta\,(\beta = 0,1,..., \frac{1}{2}N - 1)$ is the index in the frequency domain. If T is the time window, ω_s is the sampling frequency, and $\omega_{\max}$ is the upper frequency limit of the desired frequency domain:

$$\begin{aligned}T &= N\cdot\Delta t = 2\pi N/\omega_s\,,\\ \omega_{\max} &= \tfrac{1}{2}N\cdot\Delta\omega = \omega_s/2\,,\\ \Delta\omega &= 2\pi/T\,.\end{aligned} \tag{19b}$$

Equation (19b) suggests that only two of the six variables T, N, ω_s, $\omega_{\max}$, Δt, and $\Delta\omega$ are required to determine the set; in our study we choose N and $\omega_{\max}$. For the pressure signal, the same procedure given by Eqs. (19a) and (19b) is followed. Now we can compute $\tilde{Q}_1(\omega)$, $\tilde{p}_i(\omega)$, and the transfer impedance, $\tilde{Z}_i(\omega)$, at the ith location:

$$\tilde{Q}_1(\omega) = S_1\tilde{a}_1(\omega)/j\omega\,, \tag{20}$$

$$\begin{aligned}\tilde{Z}_i(\omega) &= \mathrm{Re}[\tilde{Z}_i(\omega)] + j\,\mathrm{Im}[\tilde{Z}_i(\omega)]\\ &= |\tilde{Z}_i(\omega)|e^{j\phi_i(\omega)}\\ &= [\tilde{G}_{pQ}(\omega)]_{i-1}/[G_{QQ}(\omega)]_{1-1}\\ &= [\tilde{p}_i(\omega)\cdot\tilde{Q}_1^*(\omega)]/[\tilde{Q}_1(\omega)\cdot\tilde{Q}_1^*(\omega)]\\ &= (j\omega S_1)[\tilde{p}_i(\omega)\tilde{a}_1^*(\omega)]/[\tilde{a}_1(\omega)\tilde{a}_1^*(\omega)]\\ &= (j\omega S_1)[\tilde{G}_{pa}(\omega)]_{i-1}/[G_{aa}(\omega)]_{1-1}\,,\\ i &= 2,3,...,n\,,\end{aligned} \tag{21}$$

where $\tilde{G}_{pa}$ and G_{aa} are the cross and auto power spectra, respectively. To determine the degree of similarity, dependence, and correlation between input a_1 and output p_i, we measure the coherence function, $\gamma_i^2(\omega)$:

$$\begin{aligned}\gamma_i^2 &= |\tilde{G}_{pa}(\omega)|^2_{i-1}/[G_{aa}(\omega)]_{1-1}\cdot[G_{pp}(\omega)]_{i-i}\,,\\ i &= 2,3,...,n,\end{aligned}$$

where

$$0 \leqslant \gamma_i^2(\omega) \leqslant 1\,. \tag{22}$$

To enhance the power spectral estimates/estimations and γ^2 we perform frequency domain averaging (number of averages = 50). At each location we measure the following: $\mathrm{Re}[\tilde{Z}_i(\omega)]$, $\mathrm{Im}[\tilde{Z}_i(\omega)]$, $|Z_i(\omega)|$, $\phi_i(\omega)$, and $\gamma_i^2(\omega)$. Note that only $\mathrm{Re}[\tilde{Z}_i(\omega)]$ and $\mathrm{Im}[\tilde{Z}_i(\omega)]$ are required for the determination of ω_r and ψ_r.

III. RESULTS AND DISCUSSION

In order to establish the validity of the modal analysis experiment, we compare experimental and theoretical results for the following example cases: I. Closed–closed tube, II. Closed–open tube, III. Symmetrical lumped parameter system, IV. Unsymmetrical lumped parameter system. All measurements have been conducted with air medium at room temperature and the total number of measurement lo-

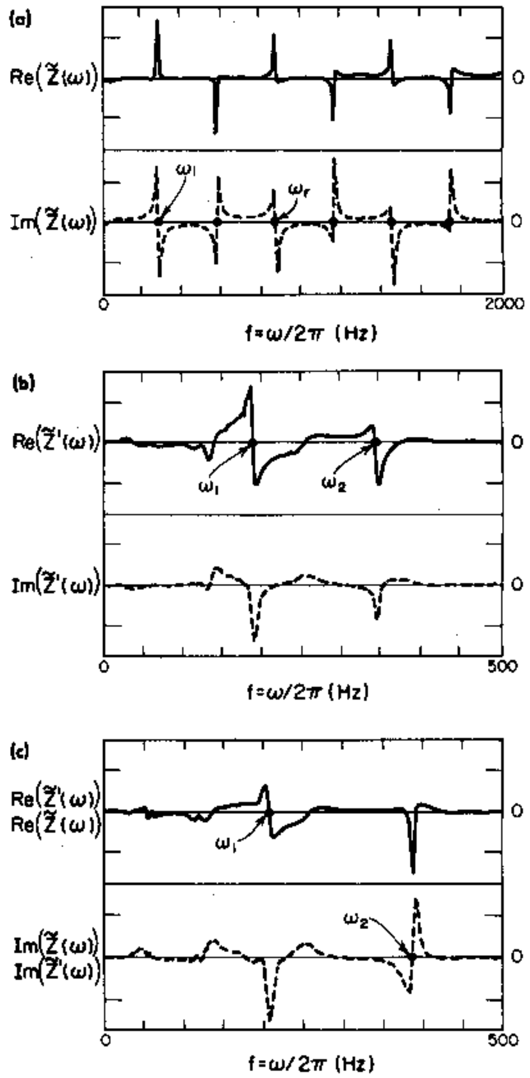

FIG. 2. Typical coincident-quadrature response curves measured for the example cases; ——— $\mathrm{Re}[\tilde{Z}_i(\omega)]$, - - - $\mathrm{Im}[\tilde{Z}_i(\omega)]$, (a) for example cases I (closed–closed tube) and II (closed–open tube), (b) for example case III (symmetrical lumped parameter system), (c) for example case IV (unsymmetrical lumped parameter system). The ordinate scale is linear and arbitrary; however, it is uniform for all locations.

cations are about 25. At any location, typical coincident-quadrature response curves are shown in Fig. 2 for the above cases. For example cases I and II, we use Eq. (15a) for finding ω_r as shown in Fig. 2(a); and Eq. (15b) is used for determining ψ_r at each natural frequency. Conversely, the other orthogonal set as given by Eq. (17) is used for example case III as shown in Fig. 2(b); Eq. (17a) for finding ω_r and Eq. (17b) for finding ψ_r at both natural frequencies. For example case IV, we use both sets given by Eqs. (15) and (17) as shown in Fig. 2(c); at ω_1, Eqs. (17a) and (17b) are used for the determination of ω_1 and ψ_1, respectively; and, at ω_2, Eqs. (15a) and (15b) are used to find ω_2 and ψ_2, respectively.

A. Example case I

For a closed–closed tube of length L containing a medium with speed of sound c, expressions for ω_r and ψ_r in the plane-wave frequency regime are[21]

$$\omega_r = r\pi c/L\,,\quad \psi_r = \cos \omega_r x/c\,,\quad r = 1,2,...,n\,. \tag{23}$$

For a cylindrical tube of length (L) 591.8 mm and diameter (d) 63.5 mm, where the first six natural frequencies are measured over the 0–2000-Hz frequency range (these values along with theoretical natural frequencies are listed and compared in Table I), note the excellent correlation with theory. Figure 3 compares the measured and predicted mode shapes associated with these natural frequencies. Again, we find excellent correlation between theory and experiment. In fact, the only discrepancies seem to be at the lower modes; these may be due to the nonlinearities associated with pressure buildup at lower frequencies because of high acoustic displacements and lack of adequate damping.

B. Example case II

For a closed–open tube of length L,

$$\omega_r = (2r-1)\pi c/2L_e\,,\quad \psi_r = \sin \omega_r x/c\,,\quad r = 1,2,...,n\,, \tag{24}$$

where L_e is the effective length given by $L + \Delta L$ with $\Delta L = 0.32d$ being the length correction at the open end.[21] For a cylindrical tube ($L = 591.8$ mm and $d = 63.5$ mm), Table I and Fig. 4 show comparison for ω_r and ψ_r, respectively. Here again, we note excellent agreement between theory and experiment.

C. Lumped parameter system

Specific cases of the lumped parameter acoustic system shown in Fig. 5 constitute example cases III and IV. For the undamped and unforced case, the equations of acoustic motion are

$$[M]\{\ddot{X}(t)\} + [K]\{X(t)\} = \begin{Bmatrix}0\\0\end{Bmatrix}\,, \tag{25}$$

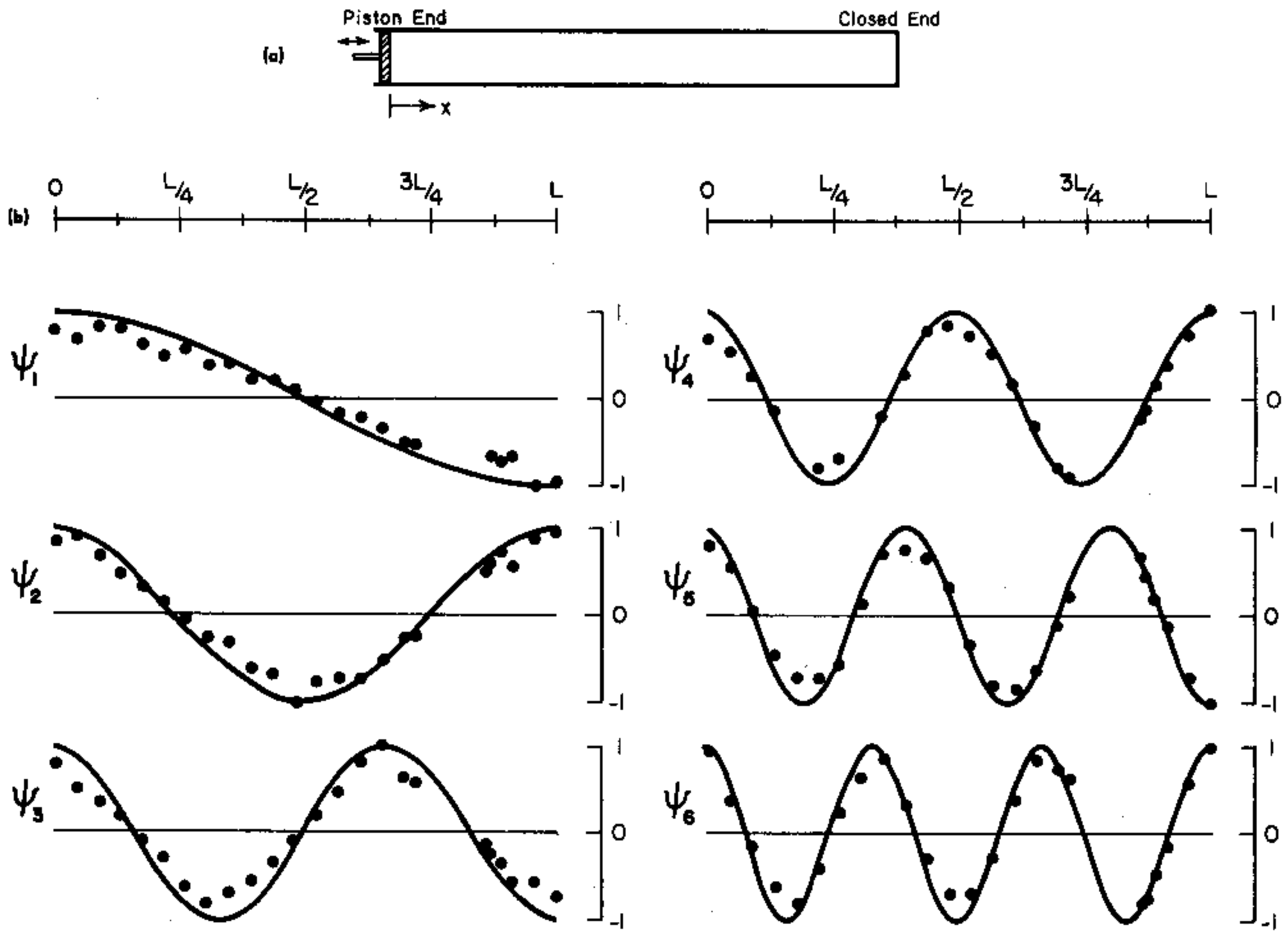

FIG. 3. (a) Example case I. (b) Pressure mode shapes ψ_r; ———theory, ···experiment.

TABLE I. Natural frequencies of example cases: experiment versus theory.

Example case	r	Medium: air at room temperature (20°–24.5 °C) $f_r = \omega_r/2\pi$, Hz Experiment[a]	Theory[b]	Comparison, %[c]
I	1	291.5	291.2	0.1
Closed–closed	2	583.0	582.5	0.08
tube	3	874.5	873.7	0.09
	4	1166.0	1165.0	0.08
	5	1457.5	1457.5	0.0
	6	1749.0	1750.0	0.05
II	1	140.9	140.0	0.64
Closed–open	2	422.6	421.2	0.33
tube	3	704.5	703.7	0.11
	4	986.3	985.0	0.13
	5	1268.1	1267.5	0.05
	6	1549.9	1550.0	0.01
III				
Symmetrical	1	191.2	200.9	4.8
lumped parameter	2	345.6	348.0	0.69
system				
IV				
Unsymmetrical	1	206.2	218.8	5.8
lumped parameter	2	385.6	396.5	2.7
system				

[a] Experimental value is the median of the sample range of measured natural frequencies.

[b] Theoretical value is the average of the natural frequencies computed at 20° and 24.5 °C room temperatures. The reason for choosing these is that an experiment was completed over a period of time under different room temperatures and equipment heating conditions.

[c] Comparison, % = 100 (experiment–theory)/theory.

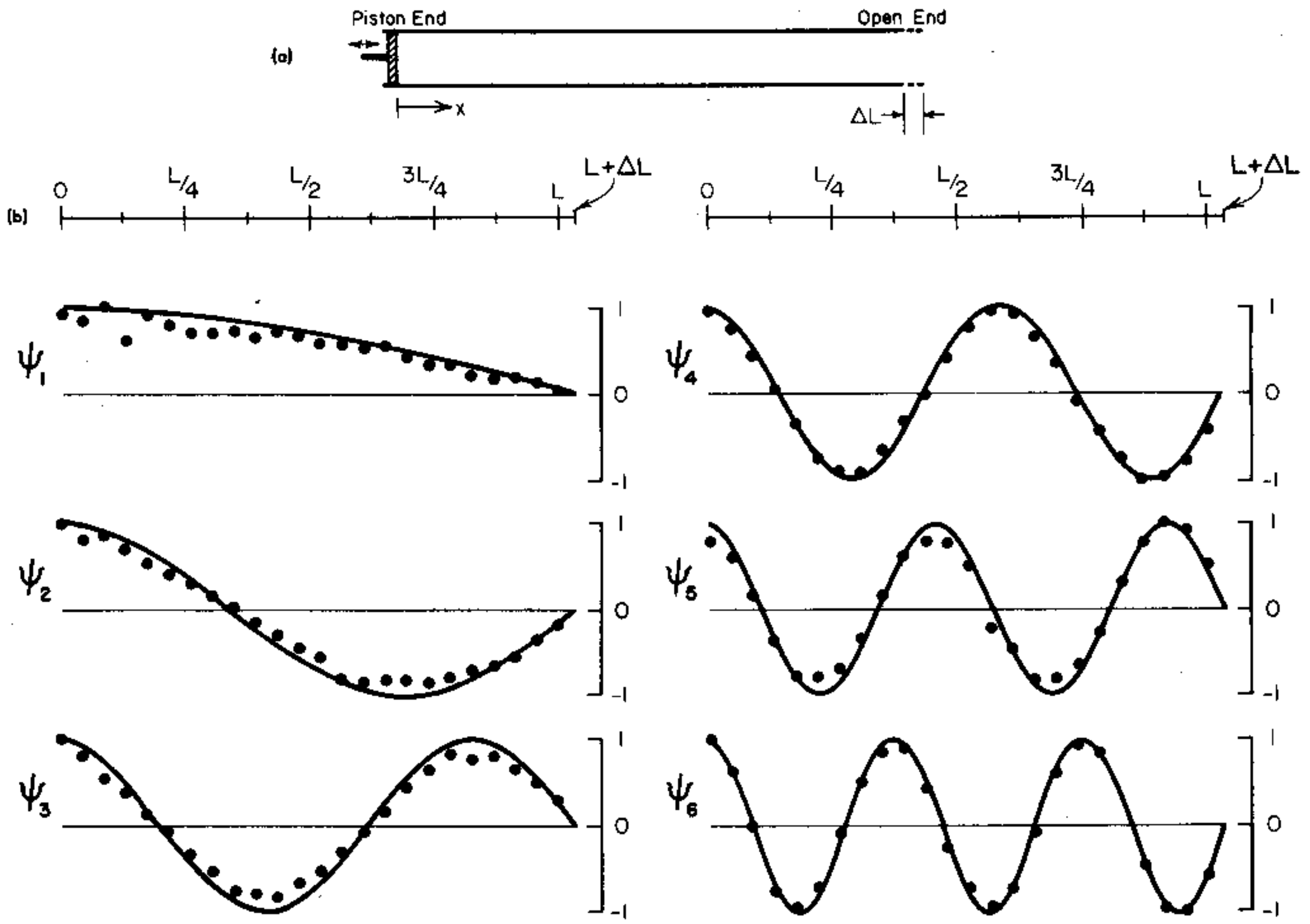

FIG. 4. (a) Example case II. (b) Pressure mode shapes ψ_r; ——— theory, ··· experiment.

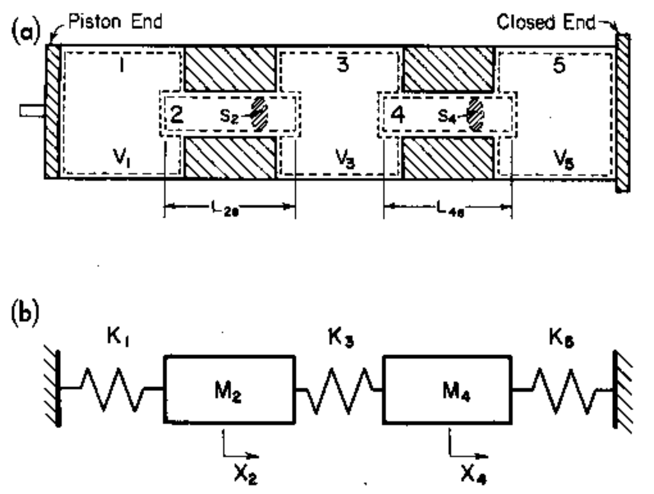

FIG. 5. Lumped parameter acoustic system. (a) Lumped acoustic elements. (b) Mechanical analog of the undamped acoustic system shown in (a).

where

$$[M] = \begin{bmatrix} M_2 & 0 \\ 0 & M_4 \end{bmatrix} = \rho \begin{bmatrix} L_{2e}/S_2 & 0 \\ 0 & L_{4e}/S_4 \end{bmatrix} \tag{26}$$

$$[K] = \begin{bmatrix} K_1 + K_3 & -K_3 \\ -K_3 & K_3 + K_5 \end{bmatrix}$$

$$= \rho c^2 \begin{bmatrix} (1/V_1) + (1/V_3) & -(1/V_3) \\ -(1/V_3) & (1/V_3) + (1/V_5) \end{bmatrix} \tag{27}$$

$$\{X(t)\} = \begin{Bmatrix} X_2(t) \\ X_4(t) \end{Bmatrix}, \tag{28}$$

where M is the acoustic mass, K is the acoustic stiffness, X is the volume displacement, and ρ is the gas medium density. For an eigenvalue solution, we assume a harmonic solution for $X(t)$. Thus the characteristic equation is

$$|[E] - \lambda [I]| = 0, \tag{29}$$

where

$$[E] = [M]^{-1}[K], \quad \lambda = \omega^2$$

and

$$[I] = \begin{bmatrix} 1 & 0 \\ 0 & 1 \end{bmatrix}. \tag{30}$$

We get two eigenvalues λ_1 and λ_2, and two eigenvectors $\{X\}_1$ and $\{X\}_2$. Thus the natural frequencies and pressure mode shapes are

$$\omega_r : \omega_r = (\lambda_r)^{1/2}, \quad r = 1,2,$$

$$\begin{aligned} \psi_r:\ & p_{1r} = K_1(X_2)_r && \text{element } \#1, \\ & p_{3r} = K_3(X_2 - X_4)_r && \text{element } \#3, \\ & p_{5r} = K_5(X_4)_r && \text{element } \#5, \\ & p_{2r} = \text{from line joining } p_{1r} \text{ and } p_{3r} && \text{element } \#2, \\ & p_{4r} = \text{from line joining } p_{3r} \text{ and } p_{5r} && \text{element } \#4. \end{aligned} \tag{31}$$

D. Example case III

Example case III is the symmetrical case of lumped parameter systems shown in Fig. 5, with the following values:

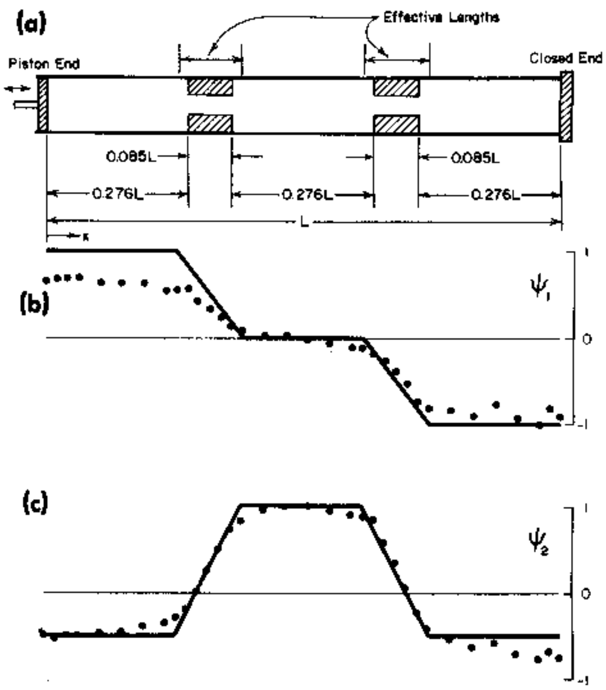

FIG. 6. Symmetrical lumped parameter system. (a) Schematic. (b) Pressure mode ψ_1. (c) Pressure mode ψ_2. For both (b) and (c) ——— theory, ··· experiment.

$$V_1 = V_3 = V_5 = 522\,858.8 \text{ mm}^3,$$

$$S_2 = S_4 = 506.7 \text{ mm}^2,$$

$$L_2 = L_4 = 50.8 \text{ mm}, \quad L_{2e} = L_{4e} = 72.39 \text{ mm},$$

and

$$\Delta L = 0.85d = 21.59 \text{ mm}.$$

For this case, the measured natural frequencies, over the 0–500-Hz range, are compared with the lumped parameter theory; we note very good correlation in spite of the simplicity of the analytical model. Theoretical modes for acoustical displacement are

$$\{X\}_1 = \begin{Bmatrix} 1 \\ 1 \end{Bmatrix}, \quad \{X\}_2 = \begin{Bmatrix} 1 \\ -1 \end{Bmatrix}. \tag{32}$$

Using Eq. (31), these are converted to the pressure modes ψ_1 and ψ_2 and plotted in Fig. 6. We again note very good correlation between experiment and lumped parameter theory except for ψ_1 near the piston end. We suspect that this is due to the nonlinearities associated with the pressure buildup especially in element 5 of Fig. 5. Also, a lack of perfect symmetry may also be responsible for the discrepancies.

E. Example case IV

Example case IV is the unsymmetrical version of the lumped parameter system of Fig. 5.

$$V_1 = V_3 = V_5 = 522\,858.8 \text{ mm}^3,$$

$$S_2 = S_4 = 506.7 \text{ mm}^2,$$

$$L_4 = 2L_2 = 50.8 \text{ mm}, \quad L_{4e} = 72.39 \text{ mm},$$

$$L_{2e} = 47.0 \text{ mm},$$

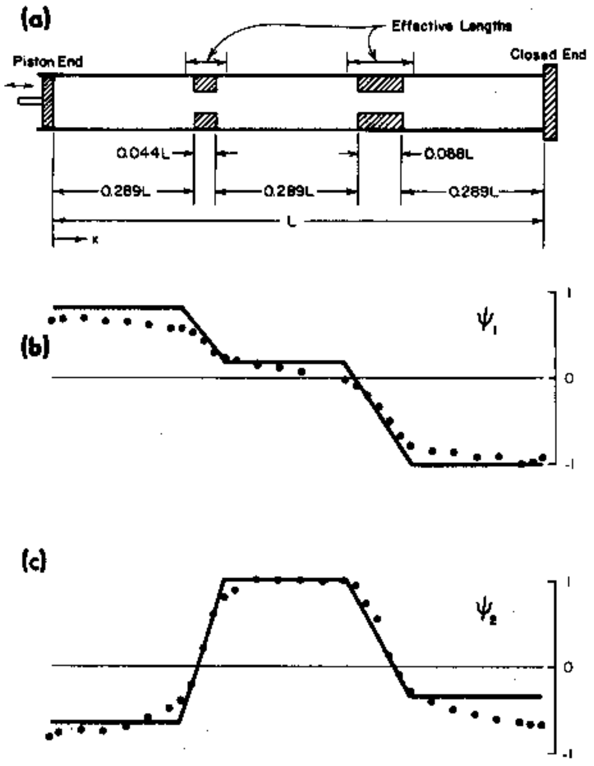

FIG. 7. Unsymmetrical lumped parameter system. (a) Schematic. (b) Pressure mode ψ_1. (c) Pressure mode ψ_2. For both (b) and (c) ——— theory, ···experiment.

and

$$\Delta L = 0.85d = 21.59 \text{ mm}.$$

For this case the measured natural frequencies are compared with lumped parameter analysis results in Table I; again note very good correlation. Theoretical modes for acoustic displacement are

$$\{X\}_1 = \begin{Bmatrix} 0.813 \\ 1.000 \end{Bmatrix}, \quad \{X\}_2 = \begin{Bmatrix} 1.000 \\ -0.528 \end{Bmatrix}. \tag{33}$$

Theoretical pressure mode shapes ψ_1 and ψ_2, as shown in Fig. 7, are compared with the measured mode shapes. Correlation between theory and experiment seems to be slightly better than the example case III. We should point out that better agreement between theory and experiment would be obtained if the distributed parameter analysis approach is used for the system shown in Fig. 5. We have, however, deliberately used the lumped parameter approach for example cases III and IV because this approach is simpler, and yields easily recognizable modal information. Thus the discrepancies are not necessarily related to the experimental method proposed in this paper.

IV. CONCLUDING REMARKS

In this paper we have proposed an experimental method of determining natural frequencies and modes for acoustic ducts over the plane-wave frequency regime. We have compared our experimental results of four example cases with theory and obtained excellent correlation. Overall, our technique for acoustic systems yields results similar to those extracted for mechanical systems. It should be pointed out that thus far we have used coincident-quadrature response curves; other methods of determining modes, such as circle fitting routine currently used for mechanical systems, should also work successfully.

Although the technique presented here has been limited to the plane-wave case and for global modal properties, it forms the basis of further work in this area, especially for three-dimensional cavities and flow ducts. Currently, we are exploring the following topics of research: (i) estimation of modal parameters such as modal acoustic mass, stiffness, and damping, (ii) modal analysis techniques applied to two- or three-dimensional acoustic ducts, (iii) extraction of mode shapes in the presence of mean fluid flow, (iv) application of two-microphone intensity measurement method to modal analysis, and (v) the study of alternate duct excitation and volume velocity measurement methods.

[1] A. L. Klosterman, "On the Experimental Determination and Use of Modal Representation of Dynamic Characteristics," Ph. D. dissertation, Univ. of Cincinnati (1971).
[2] A. Berman and W. G. Flannelly, "Theory of Incomplete Models of Dynamic Structures," Am. Inst. Aero. Astron. J. **9**, 1481–1487 (1971).
[3] M. Richardson and R. Potter, "Identification of the Modal Properties of an Elastic Structure from Measured Transfer Function Data," Instrum. Soc. Am. ASI **74250**, 239–240 (1974).
[4] M. Richardson, "Modal Analysis Using Digital Test Systems," Seminar on Understanding Digital Control and Analysis in Vibration Test Systems, Shock and Vibration Information Center, Washington DC **2**, 43–64 (1975).
[5] A. L. Klosterman, W. A. McCleland, and J. E. Sherlock, "Dynamic Simulation of Complex Systems Utilizing Experimental and Analytical Techniques," ASME Paper No. 75-WA/Aero-9 (1975).
[6] M. Richardson and J. Kniskern, "Identifying Modes of Large Structures from Multiple Input and Response Measurements," SAE Paper **760875** (1976).
[7] E. L. Peterson and A. L. Klosterman, "Obtaining Good Results from an Experimental Modal Survey," J. Soc. Environ. Eng. (March 1978).
[8] M. Rades, "Analysis Techniques of Experimental Frequency Response Data," Shock Vib. Dig. **11** (2), 11 (1979).
[9] M. A. Lamontia, "Dynamic Modeling of Engine-Block Components," Master of Science thesis, Mech. Eng., The Ohio State Univ. (1979).
[10] H. G. D. Goyder, "Methods and Application of Structural Modeling from Measured Structural Frequency Response Data," J. Sound Vib. **68** (2), 209–230 (1980).
[11] D. L. Brown and R. J. Allemang, "Modal Analysis Techniques Applicable to Acoustic Problem Solution," INTER-NOISE 78 Proc. 909–914 (1978).
[12] R. J. Allemang and W. R. Shapton, "Using Modal Techniques to Guide Acoustic Signature Analysis," Soc. Auto. Eng. Paper **780106** (1980).
[13] R. Singh, "Acoustic Impedance Measurement Methods," Shock Vib. Dig. **14**(2), 3–9 (1982).
[14] American Society of Testing Materials, "Impedance and Absorption of Acoustical Materials by the Tube Method," ASTM C384–58 (1972).
[15] C. J. Moore, "Measurement of Radial and Circumferential Modes in Annular and Circumferential Fan Ducts," J. Sound Vib. **62** (2), 235–256 (1979).
[16] R. Singh and W. Soedel, "An Efficient Method of Measuring Impedances of Fluid Machinery Manifolds," J. Sound Vib. **56**, 105–125 (1978).
[17] R. Singh and M. Schary, "Acoustic Impedance Measurement Using Sine Sweep Excitation and Known Volume Velocity Technique," J. Acoust. Soc. Am. **64**, 995–1005 (1978).
[18] D. H. Keefe and A. H. Benade, "Impedance Measurement Source and Microphone Proximity Effects," J. Acoust. Soc. Am. **69**, 1489–1495 (1981).
[19] J. S. Bendat and A. G. Piersol, *Random Data: Analysis and Measurement Procedures* (Wiley–Interscience, New York, 1971).
[20] A. F. Seybert and B. Soenarko, "Error Analysis of Spectral Estimates with Application to the Measurement of Acoustic Parameters Using Random Sound Fields in Ducts," J. Acoust. Soc. Am. **69**, 1190–1199 (1981).
[21] S. N. Rschevkin, *A Course of Lectures on the Theory of Sound* (Pergamon, Oxford, 1963), Chaps. V and VII.